INFECTION AND IMMUNITY, Feb. 2000, p. 716–724 Vol. 68, No. 2
0019-9567/00/$04.00+0

Enzymatic Properties of Dipeptidyl Aminopeptidase IV Produced by the Periodontal Pathogen *Porphyromonas gingivalis* and Its Participation in Virulence

YUMI KUMAGAI,[1]* KIYOSHI KONISHI,[1] TOMOHARU GOMI,[2] HISAO YAGISHITA,[3] AYAKO YAJIMA,[1] AND MASANOSUKE YOSHIKAWA[1]

Department of Microbiology[1] and Department of Pathology,[3] Nippon Dental University, Fujimi 1-9-20, Chiyoda-ku, Tokyo 102-8159, and Scientific Instrument Center, Toyama Medical and Pharmaceutical University, Sugitani, Toyama 930-0152,[2] Japan

Received 19 July 1999/Returned for modification 14 September 1999/Accepted 30 October 1999

***Porphyromonas gingivalis* is a major pathogen associated with adult periodontitis. We cloned and sequenced the gene (*dpp*) coding for dipeptidyl aminopeptidase IV (DPPIV) from *P. gingivalis* W83, based on the amino acid sequences of peptide fragments derived from purified DPPIV. An *Escherichia coli* strain overproducing *P. gingivalis* DPPIV was constructed. The enzymatic properties of recombinant DPPIV purified from the overproducer were similar to those of DPPIV isolated from *P. gingivalis*. The three amino acid residues Ser, Asp, and His, which are thought to form a catalytic triad in the C-terminal catalytic domain of eukaryotic DPPIV, are conserved in *P. gingivalis* DPPIV. When each of the corresponding residues of the enzyme was substituted with Ala by site-directed mutagenesis, DPPIV activity significantly decreased, suggesting that these three residues of *P. gingivalis* DPPIV are involved in the catalytic reaction. DPPIV-deficient mutants of *P. gingivalis* were constructed and subjected to animal experiments. Mice injected with the wild-type strain developed abscesses to a greater extent and died more frequently than those challenged with mutant strains. Mice injected with the mutants exhibited faster recovery from the infection, as assessed by weight gain and the rate of lesion healing. This decreased virulence of mutants compared with the parent strain suggests that DPPIV is a potential virulence factor of *P. gingivalis* and may play important roles in the pathogenesis of adult periodontitis induced by the organism.**

Porphyromonas gingivalis, a gram-negative anaerobic bacterium, is thought to be a major etiologic agent associated with adult periodontitis (13, 15). It produces several proteases, two Arg-specific cysteine proteases and a Lys-specific one, dipeptidyl aminopeptidase IV (DPPIV), prolyl tripeptidyl peptidase (PtpA), and others (1, 4, 26, 32). Arg-specific proteases have been implicated in the pathogenesis of adult periodontitis, as shown by genetic approaches (12, 28, 29, 37, 39).

DPPIV (EC 3.4.14.5) is a serine protease that cleaves X-Pro or X-Ala dipeptide from the N-terminal ends of polypeptide chains. DPPIV activity has been found in eukaryotes as well as in bacteria. The genes coding for DPPIV have been cloned and sequenced for some of these organisms (e.g., human [7, 25, 38], mouse [22], *Saccharomyces cerevisiae* [2, 35], *Chryseobacterium* [formerly *Flavobacterium*] *meningosepticum* [17]), and *P. gingivalis* [18]).

Eukaryotic DPPIV has been reported to be associated with several biological functions—e.g., (i) T-cell activation (3, 22, 27, 38, 43), (ii) binding to adenosine deaminase (ADA) (3, 10, 11, 16, 27, 43), and (iii) interaction with collagen and/or fibronectin (3, 6, 33)—as well as with the pathogenesis of diseases, such as AIDS, breast cancer, and diabetes (3, 6, 14, 31, 45). In contrast, the physiological and pathological functions of bacterial DPPIV have not been clarified.

Destruction of periodontal tissue is a critical feature of adult periodontitis. Type I collagen, one of the major components of periodontal tissue, is composed predominantly of Gly-Pro-X. *P. gingivalis* DPPIV has been suggested to contribute to the degradation of collagen, based on the fact that partially purified DPPIV possessed the activity of releasing the Gly-Pro peptide from *Clostridium histolyticum* collagenase-treated type I collagen (1). However, the detailed mechanism by which DPPIV participates in the destruction of collagen remains unclear. Considering the functions of eukaryotic DPPIV, *P. gingivalis* DPPIV was supposed to have some biological roles or to be pathologically associated with periodontitis. In the present study, we demonstrate through animal experiments with DPPIV-deficient mutants that *P. gingivalis* DPPIV is a potential virulence factor.

* Corresponding author. Mailing address: Department of Microbiology, Nippon Dental University, Fujimi 1-9-20, Chiyoda-ku, Tokyo 102-8159, Japan. Phone: 81-3-3261-8763. Fax: 81-3-3264-8399. E-mail: yumi-mic@tokyo.ndu.ac.jp.

MATERIALS AND METHODS

Bacterial strains and media. The bacterial strains used in this study are described in Table 1. *P. gingivalis* was grown anaerobically (80% N_2, 10% CO_2, 10% H_2) in brain heart infusion (BHI) broth (Difco, Detroit, Mich.) or on BHI agar plates supplemented with 5 μg of hemin (Sigma-Aldrich, St. Louis, Mo.) per ml and 0.5 μg of menadione (Sigma-Aldrich) per ml. For animal experiments, *P. gingivalis* was grown as previously described (12). *Escherichia coli* was grown in Luria-Bertani (LB) broth or on LB agar plates. SY327λ*pir* (24), λ*pir* lysogen of SY327, was the host for transformation with plasmids containing the R6K replicon, pGP704 (24), and its derivatives. SM10λ*pir* (24) was used for conjugal transfer of pGP704 derivatives. BL21 (36) was the host for pTD-T7 (8) and its derivatives, and DH1 (36) was the host for transformation with other plasmids. Antibiotics were used at the following concentrations for *E. coli*: ampicillin sodium salt (Sigma-Aldrich), 50 μg/ml; kanamycin sulfate (Sigma-Aldrich), 50 μg/ml; erythromycin (Sigma-Aldrich), 300 μg/ml; and gentamicin sulfate (Sigma-Aldrich), 100 μg/ml. For *P. gingivalis*, 10 μg of erythromycin per ml was added as required.

Purification of DPPIV from *P. gingivalis* W83. DPPIV activity was measured with 0.5 mM glycylprolyl *p*-nitroanilide (Gly-Pro-pNA) (Peptide Institute, Inc., Osaka, Japan) as a substrate in 20 mM potassium phosphate buffer (pH 7.5) at 25°C, and released *p*-nitroaniline was spectrophotometrically monitored at 405 nm. *P. gingivalis* W83 was harvested at the stationary phase. Cells were washed with 10 mM potassium phosphate–1 mM EDTA buffer (pH 7.5), resuspended in

TABLE 1. List of strains and plasmids

Strain or plasmid	Description[a]	Source or reference
Strains		
Porphyromonas gingivalis		
W83		Laboratory stock
4351	W83 Δ*dpp*	Present study
4361	W83 Δ*dpp*	Present study
EM23	W83 *dpp*::ϕ (*ermF-ermAM*)	Present study
Escherichia coli		
SY327λ*pir*	Δ(*lac pro*) *argE*(Am) *rif nalA recA56 pir*	24
SM10λ*pir*	*thi thr leu tonA lacY supE recA*::RP4-2-Tc::Mu Km *pir*	24
BL21	*hsdS gal* (λ*c*I*ts*857 *ind*1 *Sam*7 *nin*5 *lac*UV5-T7 gene*1*)	36
DH1	*supE44 hsdR17 recA1 endA1 gyrA96 thi-1 relA1*	36
DPPRWT	BL21/pYKP406	Present study
DPPRSA	BL21/pYKP407	Present study
DPPRDA	BL21/pYKP408	Present study
DPPRHA	BL21/pYKP409	Present study
Plasmids		
pUC119	Ap^r	36
pUC4K	Ap^r Km^r	42
pGP704	*ori*R6K *mob*RP4 Ap^r	24
pTD-T7	Ap^r T7 promoter	8
pYKP001	pVA2198 Km^r	Present study
pYKP002	pGP704 ϕ(*ermF-ermAM*) Ap^s	Present study
pYKP009	pGP704 ϕ(*ermF-ermAM*) Ap^s; one *Sph*I site was eliminated	Present study
pYKP200	pYKP009 ALAR fragment	Present study
pYKP300	pBR322 *dpp*	Present study
pYKP301	pYKP300 *dpp*::ϕ (*ermF-ermAM*)	Present study
pYKP403	pTD-T7 *dpp* coding for DPPIV with a putative signal sequence	Present study
pYKP406	pTD-T7 *dpp* coding for DPPIV without a putative signal sequence	Present study
pYKP407	pTD-T7 *dpp* expressing S593A	Present study
pYKP408	pTD-T7 *dpp* expressing D668A	Present study
pYKP409	pTD-T7 *dpp* expressing H700A	Present study

[a] Ap^r, ampicillin resistant; Ap^s, ampicillin sensitive; Km^r, kanamycin resistant, *ori*R6K, replication origin of plasmid R6K; *mob*RP4, *oriT* region of plasmid RP4.

the same buffer, frozen-thawed, sonicated with an Ultrasonic Generator (Nihonseiki, Tokyo, Japan), and centrifuged at 70,000 × *g* for 1 h. The resulting supernatant was fractionated on a DEAE-Sephacel column (Amersham Pharmacia, Little Chalfont, United Kingdom) that had been equilibrated with 10 mM potassium phosphate–1 mM EDTA buffer (pH 7.5). Retained proteins were eluted with a linear gradient of 50 to 120 mM NaCl in 10 mM potassium phosphate–1 mM EDTA buffer (pH 7.5). Pooled active fractions were concentrated with an Ultrafree C3-LGC centrifugal filter unit (Millipore, Bedford, Mass.) and applied to a Sephacryl S-300 HR column (Amersham Pharmacia) that had been equilibrated with 20 mM potassium phosphate–100 mM NaCl–1 mM EDTA buffer (pH 7.5), followed by elution with the same buffer. Ammonium sulfate was added to the pooled active fractions at a final concentration of 1.5 M (35% saturation), and the fractions were then applied to a butyl-Sepharose column (Amersham Pharmacia) that had been equilibrated with 10 mM potassium phosphate–1 mM EDTA–1.5 M ammonium sulfate buffer (pH 7.5), followed by elution with a linear gradient of 1.5 to 0 M ammonium sulfate in 10 mM potassium phosphate–1 mM EDTA buffer (pH 7.5). Combined active fractions were finally applied to a hydroxyapatite column (Bio-Rad, Hercules, Calif.) that had been equilibrated with 150 mM potassium phosphate buffer (pH 7.5), and retained proteins were eluted with a linear gradient of 150 to 300 mM phosphate buffer (pH 7.5). The purity of proteins was confirmed by sodium dodecyl sulfate (SDS)-polyacrylamide gel electrophoresis (PAGE) (20). The protein concentration was determined with bovine serum albumin as a standard by use of the BCA (bicinchoninic acid) Protein Assay Kit (Pierce, Rockford, Ill.).

DNA manipulation. DNA was extracted from agarose gels with the Geneclean II Kit (Bio 101, Inc., Vista, Calif.). Transformation of *E. coli* with plasmids was performed by electroporation with a Gene Pulser II (Bio-Rad). Preparation of DNA probes, colony hybridization, and Southern hybridization were carried out with the DIG (digoxigenin) DNA Labeling and Detection Kit (Boehringer GmbH, Mannheim, Germany). A series of deletion mutants for DNA sequencing were prepared with the Kilo-Sequence Deletion Kit (TaKaRa, Kusatsu, Japan). Sequencing was performed with the AutoRead Sequencing Kit (Amersham Pharmacia), followed by analysis with an A.L.F.DNA Sequencer (Amersham Pharmacia). Other methods were as described previously (36).

Isolation and sequencing of the gene coding for DPPIV. When we began and completed sequencing the gene coding for DPPIV, no sequence information was available for DPPIV from any strains of *P. gingivalis*, including 381 (18) and W83. Therefore, we used amino acid sequences of the purified enzyme to obtain information for cloning. The N-terminal amino acid sequence could not be determined after several attempts. Instead, internal amino acid sequences were determined as follows. The purified enzyme was digested with lysyl endopeptidase (Wako, Osako, Japan) at a 200:1 (mol/mol) ratio at 25°C for 20 h, and the resulting peptides were isolated by reverse-phase high-pressure liquid chromatography (HPLC) (ODS-120T; Tosoh, Tokyo, Japan) with a linear gradient of 0 to 80% acetonitrile in 0.1% trifluoroacetic acid at a flow rate of 0.7 ml/min. The sequences of the nine fragments were automatically determined with a PPSQ-10 gas-phase peptide sequencer system (Shimadzu, Kyoto, Japan). Since two of the nine peptides exhibited high homology with other eukaryotic DPPIVs in a search of the GenBank/EMBL/DDBJ database, primers for PCR were designed based on the sequences of the peptide fragments as follows: 5′-CCGGATCCGA(C/T)GG(A/C/G/T)(A/C/T)G(A/C/G/T)ATGGT(A/C/G/T)GC-3′, containing a *Bam*HI site (underlined), and 5′-GGCTGCAGTC(G/A)TA(G/A)AA(A/C/G/T)C(T/G)CCA(G/A)TC(A/C/G/T)GC-3′, containing a *Pst*I site (underlined). PCR was performed with *P. gingivalis* W83 chromosomal DNA as the template. The resulting 1.5-kbp PCR fragment was used as a probe to screen a plasmid library made by partially digesting *P. gingivalis* chromosomal DNA with *Mbo*I and ligating the DNA to pUC119 digested with *Bam*HI by colony hybridization. Three overlapping DNA fragments derived from a single gene, as demonstrated by restriction endonuclease analysis, were isolated. Southern blotting revealed that one copy of the gene exists on the chromosome (data not shown). We combined the sequence data for the three clones and obtained a complete sequence.

Construction of *E. coli* strains harboring expression vectors for *P. gingivalis* wild-type DPPIV protein and mutant proteins. A DNA fragment containing the *dpp* gene was generated by PCR with W83 chromosomal DNA as the template and with the following primers: ML1, 5′-GGGTCGACCATCGTAACCATGTGTGCC-3′, with a *Sal*I site (underlined) beginning at base 33 from the translation initiation codon, and OPR3, 5′-CCGCATGCCTGTATTAAAGATTGTC

G-3′, with an *Sph*I site (underlined) ending 5 bp downstream from the stop codon. The resulting PCR fragment was digested with *Sal*I and *Sph*I and ligated to *Sal*I- and *Sph*I-digested pTD-T7 (8) to yield pYKP403. To construct the plasmid for overproducing wild-type DPPIV, pYKP406, "loop-out" mutagenesis was performed by the Kunkel method (19) with primer DP4MQ-2 (5′-TTTGT TCCCCGTCTGCATAGCTGTTTCCTG-3′) according to the instruction manual for Mutan-K (TaKaRa). BL21 was transformed with pYKP406 to create strain DPPRWT. pYKP407 for producing mutant DPPIV protein S593A, pYKP408 for producing D668A, and pYKP409 for producing H700A were created by the Kunkel method (19) with primers DPP4S (5′-GCCGCCATAGG CCCACCCCCA-3′), DPP4D (5′-AACATTGTCGGCTGCCGATCC-3′), and DPP4H-2 (5′-CCCGTATATACTAGCGTTCTTGTCCAT-3′), respectively. BL21 was transformed with these plasmids to produce strains DPPRSA, DPPRDA, and DPPRHA, respectively (Table 1).

Purification of DPPIV from the overproducers. A 1/20 portion of overnight cultures of *E. coli* overproducers was added to LB broth without glucose and incubated aerobically at 30°C for 3 h. Isopropyl-β-D-thiogalactopyranoside (IPTG) was added to each culture at a final concentration of 0.1 mM, and the cultures were incubated aerobically at 30°C for 4 h. Cells were harvested, resuspended in 10 mM Tris-HCl buffer (pH 7.5), frozen-thawed, sonicated with an Ultrasonic Generator, and centrifuged at 15,000 × *g* for 30 min. The resulting supernatant was diluted threefold and subjected to chromatography on a hydroxyapatite column equilibrated with 0.2 M Tris-HCl buffer (pH 7.5). After the column was washed with the same buffer, retained proteins were eluted with a linear gradient of 0.2 to 0.6 M Tris-HCl buffer (pH 7.5). The protein concentration and kinetic constants of the purified enzyme were determined.

Antiserum against *P. gingivalis* DPPIV was prepared by immunizing a rabbit with the wild-type DPPIV sample purified from strain DPPRWT as an antigen according to a previously described method (36). Western blotting was performed as described previously (36).

Binding of DPPIV to ADA. Binding of *P. gingivalis* DPPIV or human DPPIV to ADA was investigated by use of modifications of the procedure described by Iwaki-Egawa et al. (16). Briefly, samples of *P. gingivalis* DPPIV or human DPPIV (1 μg) were incubated with calf intestine mucosa ADA (1 μg) (Sigma-Aldrich) for 30 min at 37°C in 10 mM Tris-HCl buffer. For electrophoresis under nondenaturing conditions, human DPPIV reaction mixtures were loaded onto a 3 to 8% Tris-acetate gel (NOVEX, San Diego, Calif.) and *P. gingivalis* DPPIV reaction mixtures were loaded onto a 50 mM Tris-HCl nondenaturing gel (pH 8.8) or onto an isoelectric focusing gel (pH 3 to 10) (NOVEX). Proteins on gels were detected by Coomassie brilliant blue (CBB) staining and by Western blotting with anti-ADA antibody and anti-*P. gingivalis* DPPIV antibody. ADA affinity column chromatography was performed as previously described (10), except for the detergents.

Construction of *dpp* mutants of *P. gingivalis*. *dpp* null mutants were constructed as depicted in Fig. 1. The *Eco*RI fragment of pUC4K (42) containing the kanamycin resistance gene was inserted into the *Eco*RI site of pVA2198 (12) to yield pYKP001. The *Pst*I fragment containing the *ermF-ermAM* cassette, which confers erythromycin resistance (Em^r) to both *P. gingivalis* and *E. coli* (12), was ligated to the *Pst*I site of suicide vector pGP704 (24). The resulting plasmid, pYKP002, was digested with *Kpn*I to eliminate one of the two *Sph*I sites and self-ligated to generate pYKP009. pYKP002 and pYKP009 possess several cloning sites, including *Sph*I and *Sac*I, and are suicide vectors transferable to *P. gingivalis* and selectable for the Em^r phenotype when inserted into *P. gingivalis* chromosomal DNA. A derivative of pYKP009, pYKP200, which possesses a fused fragment ALAR of the flanking regions with the reading frame of *dpp* deleted (Fig. 1A), was created to construct null mutants.

The fragment containing the flanking regions was generated by PCR with *P. gingivalis* W83 chromosomal DNA as the template. The AL fragment (463 bp), located upstream of *dpp* (positions −511 to −49 from the translation initiation codon), was generated with primer AL1, 5′-GGGCATGCTATCCACAACTAT GAAAGAG-3′, with an *Sph*I site (underlined), and primer AL2, 5′-CCCAGC TGCAATGCACGATCCATCTCTC-3′, with a *Pvu*II site (underlined). The AR fragment (422 bp), located downstream of the *dpp* gene, including 135 bp of the 3′ coding region, was amplified with primer AR1, 5′-GGCAGCTGACAGAGG CACTGGTTCAGGC-3′, containing a *Pvu*II site (underlined), and primer AR2, 5′-CCGAGCTCATCACCACCGATCATGAAGG-3′, containing a *Sac*I site (underlined). The AL and AR fragments were digested with *Sph*I/*Pvu*II and *Sac*I/*Pvu*II, respectively. PCR was performed with a mixture of both the AL and the AR fragments as templates and with primers AL1 and AR2. The resulting ALAR fragment was digested with *Sph*I and *Sac*I and ligated with *Sph*I- and *Sac*I-digested pYKP009 to yield pYKP200 (Fig. 1A).

SM10λ*pir* was transformed with pYKP200, and the plasmid was then transferred to *P. gingivalis* W83 by selection with erythromycin and counterselection with gentamicin as described elsewhere (28), with some modifications. Em^r transconjugants of *P. gingivalis* W83 thus formed were purified and grown successively in BHI broth to obtain erythromycin-sensitive (Em^s) colonies, which were then purified and examined by PCR, Southern hybridization, and Western blotting to confirm that the fragment consisting of the vector and the *dpp* gene had been lost. Two null mutants, 4351 and 4361, were thus isolated.

The *dpp* gene insertion mutant, EM23, was constructed as shown in Fig. 2. The *Eco*RV fragment containing the *dpp* gene was cloned from W83 chromosomal DNA by colony hybridization with pBR322 as the vector to create pYKP300. The *Pst*I fragment of pYKP001 mentioned above (Fig. 1A) and containing the *ermF-ermAM* cassette was ligated with pYKP300 digested with *Eco*T22I, resulting in pYKP301. pYKP301 was linearized by *Eco*RV digestion, and the *Eco*RV fragment containing both the *dpp* gene and the *ermF-ermAM* cassette was introduced into *P. gingivalis* W83 by electroporation as previously described (12). Erythromycin was used as a selection marker instead of clindamycin. Except for spontaneous mutants, Em^r colonies should have arisen only when the *ermF-ermAM* cassette was inserted into the *dpp* gene on the chromosome as a result of a double-crossover event, since the introduced DNA cannot replicate in W83 (Fig. 2B). Em^r transformants thus obtained were purified and confirmed to have no DPPIV activity. One of the mutants was designated EM23.

Animal experiments. W83 and DPPIV-deficient mutants were grown until the early stationary phase. The growth phase was judged by measuring the optical densities of cultures. Cells were harvested and washed with phosphate-buffered saline, and W83 and the mutants were adjusted to the same cell concentrations in phosphate-buffered saline. Numbers of viable cells were counted by spreading the cultures on BHI agar plates, and we confirmed the absence of contamination. BALB/c mice (11 weeks) were challenged with a dorsal subcutaneous injection of 0.2 ml of bacterial suspension. General health, weight, and presence and location of lesions were assessed daily. Statistical significance of differences in lesion formation and lethality caused by injection of W83 and mutant strains was examined by Fisher's exact probability test.

Nucleotide sequence accession number. The DDBJ accession no. assigned to the *dpp* gene of *P. gingivalis* W83 is AB008194.

RESULTS

Purification and characterization of DPPIV protein from *P. gingivalis*. More than 90% of the DPPIV activity was found in the supernatant (hereafter referred to as the soluble fraction) after sonication and centrifugation. No DPPIV activity was found in the culture fluids. The enzyme was purified to about 1,000-fold from the soluble fraction and reached homogeneity (Fig. 3A). Nineteen micrograms of the purified enzyme was obtained from 1.5 liters of bacterial culture.

The purified enzyme exhibited a 78-kDa single band in SDS-PAGE. When the sample was chromatographed on an HPLC gel filtration column (TSK gel G3000SWXL; Tosoh) under nondenaturing conditions, the retention time was at a position corresponding to a molecular mass of 140 kDa (data not shown). The K_m and V_{max} values were estimated to be 0.28 mM and 18 μmol/min/mg, respectively, with Gly-Pro-pNA as a substrate. The range of optimum pH of the enzyme was 7.5 to 8.5, with the highest activity occurring at pH 8.0. After incubation at 50°C for 30 min, 70% of the enzyme activity remained. DPPIV activity was not affected by 5 mM dithiothreitol.

Isolation and sequencing of the gene coding for DPPIV. By the methods described in Materials and Methods, we isolated and sequenced the gene coding for DPPIV, designated *dpp*, which was composed of a coding region of 2,169 nucleotides. The open reading frame encodes a protein of 723 amino acids with a calculated molecular mass of 81.8 kDa. This value is in good agreement with that estimated by SDS-PAGE (78 kDa). The deduced amino acid sequence contains sequences of the nine peptides derived from purified DPPIV and mentioned in Materials and Methods.

The amino acid sequence exhibits high homology with those of other DPPIVs—about 30% identical to human DPPIV (7, 25, 38) and mouse DPPIV (22) and 43% identical to *C. meningosepticum* DPPIV (17). Serine proteases and serine esterases share a Gly-X-Ser-X-Gly consensus motif found around the active serine (5). This motif occurs in the C-terminal catalytic domain of other DPPIVs (21) with the consensus sequence Gly-Trp-Ser-Tyr-Gly. Three residues, Ser624, Asp702, and His734, are thought to form a catalytic triad in mouse DPPIV (9). The consensus motif around the active Ser and the three amino acids corresponding to the catalytic triad are found in *P. gingivalis* DPPIV from alignment data. The putative catalytic triad in *P. gingivalis* DPPIV is Ser593, Asp668, and His700. On the other hand, no significant homology with other bacterial peptidases, such as *Lactococcus* (23, 30) and

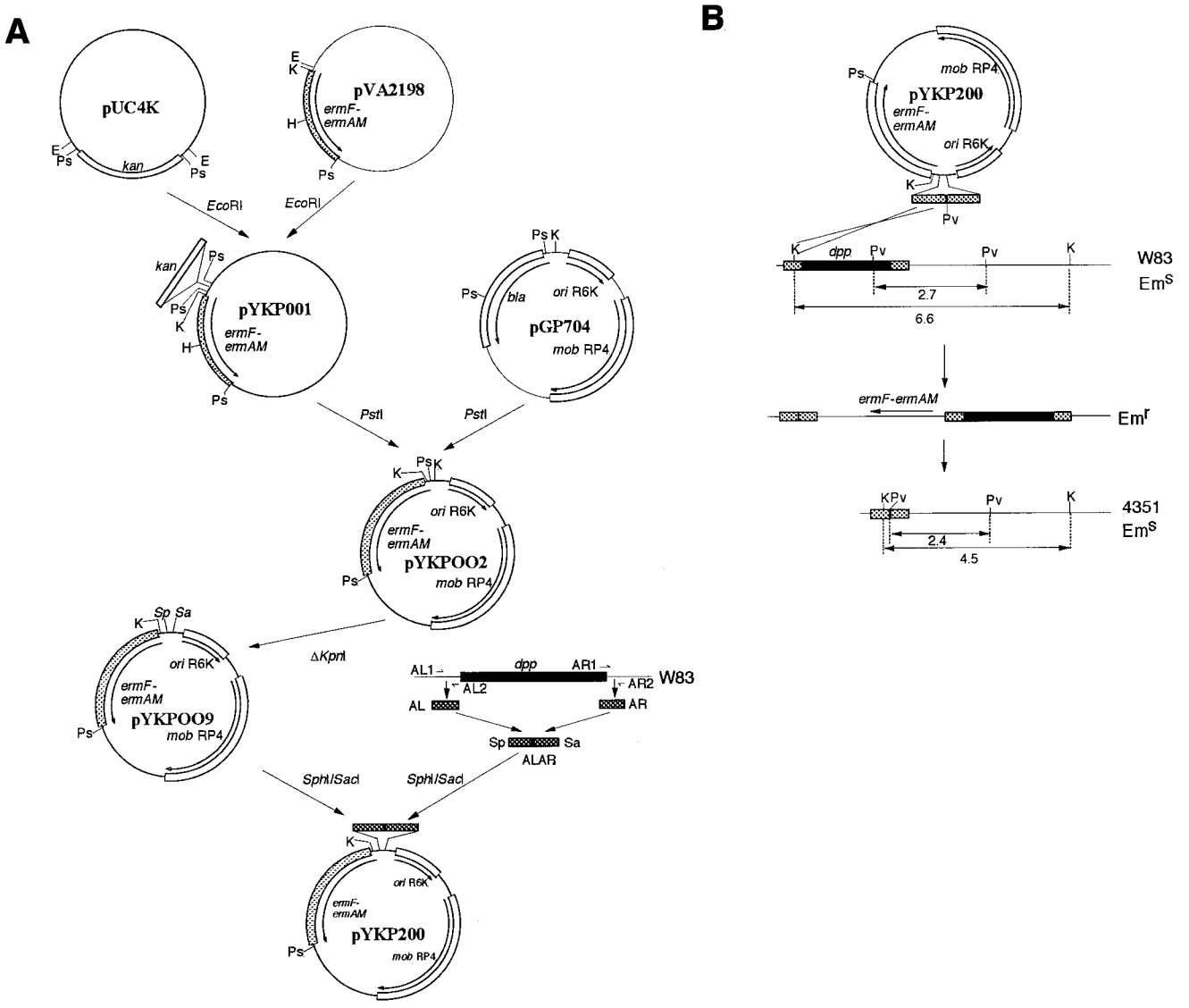

FIG. 1. Isolation of *dpp* null mutants. (A) Construction of plasmid pYKP200. Details are described in Materials and Methods. (B) One of the recombination events leading to *dpp* null mutants. Lengths of restriction fragments are shown in kilobases. Abbreviations: *kan*, the aminoglycoside 3′-phosphotransferase gene conferring kanamycin resistance; *bla*, the β-lactamase gene; *ori* R6K, replication origin of plasmid R6K; *mob* RP4, *oriT* region of plasmid RP4; E, *Eco*RI; H, *Hin*dIII; K, *Kpn*I; Ps, *Pst*I; Pv, *Pvu*II; Sa, *Sac*I; Sp, *Sph*I; Em^r, erythromycin resistant; Em^s, erythromycin sensitive.

Lactobacillus (41) X-Pro dipeptidyl aminopeptidases, was found, except for a few residues around the active Ser and the residues of the catalytic triad, even though the enzymatic activities of the peptidases are the same as those of DPPIV.

Enzymatic properties of recombinant DPPIV. The amino acid sequence deduced from the *dpp* gene contains a typical signal sequence in its N terminus. The signal sequence consists of three domains, N, H, and C (34). Lys and Arg residues are found in the N domain, the H domain is composed predominantly of hydrophobic residues, and one Gly residue is found in the H domain. When the (−3, −1) rule of von Heijne (44) is applied to the N-terminal sequence of *P. gingivalis* DPPIV, the enzyme is predicted to be cleaved between residue 19 (Ala) and residue 20 (Gln) upon secretion, since residue 19 Ala (−1) and residue 17 Ala (−3) are in good agreement with the (−3, −1) rule. We constructed an *E. coli* strain expressing *P. gingivalis* DPPIV protein whose second amino acid after the initiation Met is Gln (residue 20 of the enzyme). The *dpp* gene was located between the codon for the initiation Met and the transcription termination signal of plasmid pTD-T7 (8), so that the gene was under the control of the T7 promoter, resulting in pYKP403. Loop-out mutagenesis was carried out to ligate the codons for the initiation Met and for residue 20 Gln to produce pYKP406. Strain DPPRWT, BL21 carrying pYKP406, was cultured, and the expression of DPPIV protein was induced by IPTG. High-level expression was observed by CBB staining (Fig. 3B) and Western blotting (data not shown). The recombinant protein was purified from the overproducer to near homogeneity (Fig. 3B). From 1 liter of bacterial culture, 7.6 mg of recombinant protein was obtained. The N-terminal amino acid sequence of the protein was Met followed by Gln, indicating that the initiation Met was not removed in *E. coli*. The K_m and V_{max} values of the recombinant protein were estimated to be 0.21 mM and 23 μmol/min/mg, respectively. The values

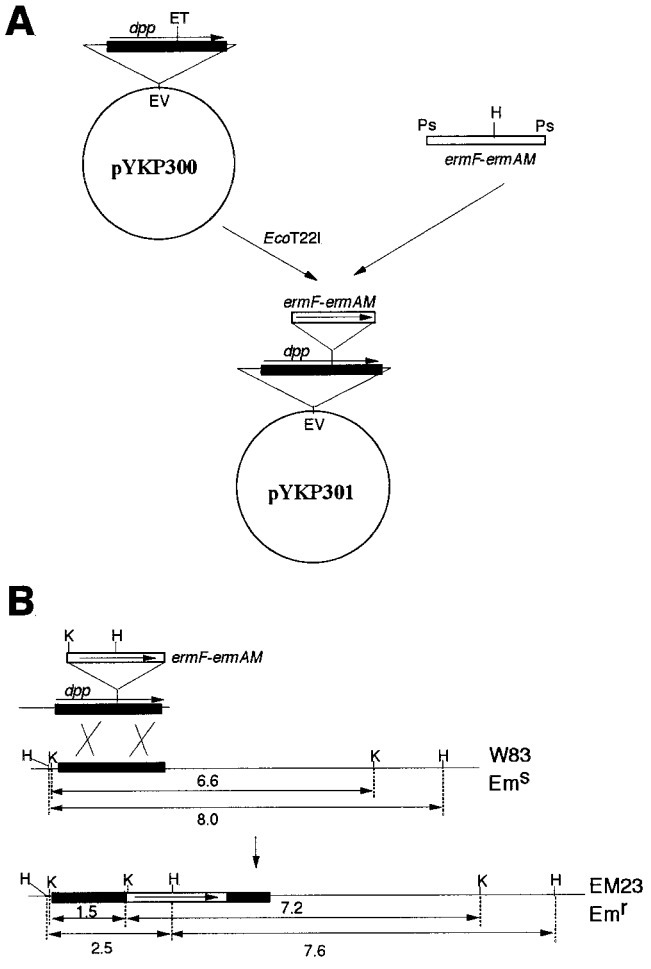

FIG. 2. Insertion mutation of the *dpp* gene. (A) Plasmid pYKP301, constructed as described in Materials and Methods. (B) Double-crossover event leading to an insertion mutation between W83 chromosomal DNA and the *Eco*RV fragment excised from pYKP301. Lengths of restriction fragments are shown in kilobases. Abbreviations: ET, *Eco*T22I; EV, *Eco*RV; H, *Hin*dIII; K, *Kpn*I; Ps, *Pst*I; Em^r, erythromycin resistant; Em^s, erythromycin sensitive.

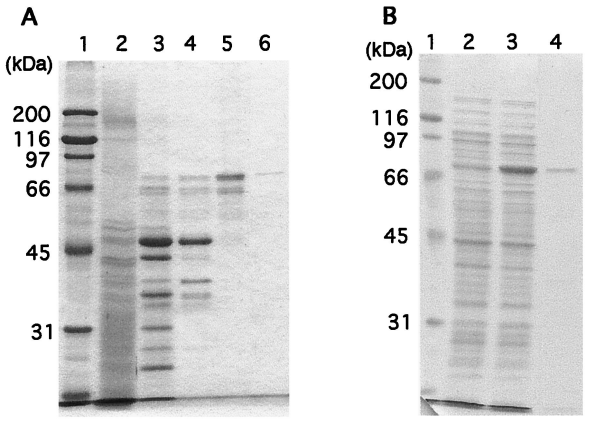

FIG. 3. CBB-stained SDS-polyacrylamide gels showing purification of DPPIV from *P. gingivalis* W83 (A) and expression and purification of recombinant DPPIV (B). (A) Lane 1, molecular mass markers; lane 2, crude extract; lane 3, DEAE-Sephacel column; lane 4, Sephacryl S-300 HR column; lane 5, butyl-Sepharose column; lane 6, hydroxyapatite column. (B) Lane 1, molecular mass markers; lanes 2 and 3, crude extracts of BL21/pTD-T7 (lane 2) and DPPRWT (BL21/pYKP406) (lane 3) harvested after incubation at 30°C for 4 h in the presence of 0.1 mM IPTG; lane 4, sample from DPPRWT after purification though a hydroxyapatite column.

were almost equal to those of DPPIV purified from *P. gingivalis*, indicating that DPPIV isolated from *P. gingivalis* and recombinant DPPIV have almost the same enzymatic properties.

Enzymatic characteristics of *P. gingivalis* DPPIV. It was reported that human DPPIV cleaved human CC chemokines (β-chemokines) at the C terminus of the Pro residue on the penultimate position of the N terminus (3, 40). Cleavage of two synthetic peptides, Ser-Pro-Tyr-Ser-Ser-Asp-Thr-Thr (corresponding to the N-terminal amino acids of human RANTES) and Gln-Pro-Asp-Ala-Ile-Asn-Ala-Pro (corresponding to the N-terminal amino acids of human MCP1), by recombinant DPPIV was examined. The recombinant enzyme cleaved the peptides in the same fashion as human DPPIV did, as demonstrated by reverse-phase HPLC with a TSK gel ODS-80Ts column (Tosoh) (data not shown).

As reported previously (16), the present study reconfirmed the ability of human DPPIV to bind to ADA. In contrast, we did not detect the binding of *P. gingivalis* DPPIV to ADA. After incubation of recombinant DPPIV and ADA, the reaction mixture was loaded onto a 50 mM Tris-HCl nondenaturing gel (pH 8.8). Under these conditions, protein bands of DPPIV and ADA were detected not only by CBB staining but also by Western blotting with anti-*P. gingivalis* DPPIV antibody and anti-ADA antibody, respectively. However, the band detected by anti-*P. gingivalis* DPPIV antibody was not stained by anti-ADA antibody. The same result was obtained when the reaction mixture was loaded onto an isoelectric focusing gel (pH 3 to 10). DPPIV purified from wild-type *P. gingivalis* W83 showed the same results (data not shown). When DPPIV from *P. gingivalis* was tested on an ADA affinity column, binding of the enzyme to the column was not observed.

Amino acid residues involved in the catalytic activity of *P. gingivalis* DPPIV. When *P. gingivalis* DPPIV was aligned with other DPPIVs, Ser593, Asp668, and His700 were suggested to participate in DPPIV activity. To explore the involvement of these three amino acid residues in catalytic function, we performed in vitro site-directed mutagenesis of *P. gingivalis* DPPIV. Each of the residues was substituted with Ala to create S593A, D668A, and H700A mutant proteins. The levels of expression of the mutant proteins in strains DPPRSA, DPPRDA, and DPPRHA were almost the same as that of the wild-type protein in strain DPPRWT. The specific activity of wild-type DPPIV was estimated to be 15 μmol/min/mg, while those of the mutant proteins were all less than 2 nmol/min/mg, with 0.4 mM Gly-Pro-pNA as a substrate. Reduction of DPPIV activity of the mutant proteins to less than 1/7,500 wild-type activity suggests that the three amino acid residues are directly involved in the catalytic reaction and that Ser593 is likely to be the catalytic Ser.

Molecular characterization of DPPIV-deficient mutants of *P. gingivalis*. To investigate the importance of DPPIV in the virulence of *P. gingivalis*, we constructed DPPIV-deficient mutants of *P. gingivalis* W83 as described in Materials and Methods. Two null mutants, 4351 and 4361, were isolated. DPPIV activity was detected in neither of them. The chromosomal DNAs of the two strains were analyzed by PCR with the primer sets primer AL1-primer AL2 and primer AL1-primer AR2 (Fig. 1A). A 463-bp fragment was amplified from both W83 and 4351 chromosomal DNAs with the primer AL1-primer AL2 set. A 2,970-bp fragment and an 885-bp fragment were

developed from W83 and 4351 chromosomal DNAs, respectively, with the primer AL1-primer AR2 set.

For Southern hybridization analysis, chromosomal DNAs of W83 and 4351 were digested with *Pvu*II or *Kpn*I. With the AR fragment (Fig. 1A) as a probe, 2.7-kbp *Pvu*II and 6.6-kbp *Kpn*I fragments from W83 DNA hybridized, while 2.4-kbp *Pvu*II and 4.5-kbp *Kpn*I fragments from 4351 DNA hybridized (Fig. 1B). For Western blotting, crude extracts prepared from W83 and 4351 were loaded onto an SDS-polyacrylamide gel, and proteins on the gel were transferred to a membrane. The anti-*P. gingivalis* DPPIV antibody stained a 78-kDa band from W83 but no band from 4351. Strain 4361 showed the same results in PCR, Southern blotting, and Western blotting as strain 4351. Taken together, these results indicate that 4351 and 4361 are null mutants with most of the *dpp* gene deleted. Mutant 4351 was chosen for further analysis.

One of the insertion mutants derived from W83, EM23 (Fig. 2), was further analyzed by Southern blotting. Chromosomal DNAs of W83 and EM23 were digested with *Kpn*I or *Hin*dIII. With the *ermF-ermAM* fragment (Fig. 2) as a probe, no hybridized band was seen with W83 DNA; on the contrary, a 7.2-kbp *Kpn*I fragment and 7.6- and 2.5-kbp *Hin*dIII fragments from EM23 DNA hybridized (Fig. 2B). With the ALAR fragment (Fig. 1) as a probe, a 6.6-kbp *Kpn*I fragment and an 8.0-kbp *Hin*dIII fragment from W83 DNA hybridized, while 7.2- and 1.5-kbp *Kpn*I fragments and 7.6- and 2.5-kbp *Hin*dIII fragments from EM23 DNA hybridized (Fig. 2B).

The growth rates of the mutants, 4351, 4361, and EM23, were similar to that of parental strain W83 in BHI broth, indicating that DPPIV is not essential for bacterial growth in rich medium.

Animal experiments. Total cell numbers, as indicated by optical densities of both wild-type W83 and the mutant strains (4351 and EM23), were proportional to viable cell numbers at both the logarithmic and the early stationary phases. In contrast, after the cells reached the stationary phase, the numbers were no longer proportional, presumably because some cells were not viable at this phase. Therefore, we harvested bacterial cells when they were determined by optical density measurements to have reached the early stationary phase. W83 or mutant (4351 or EM23) cells were injected subcutaneously into the dorsal surface of mice. There was no significant decrease in viable cell numbers due to exposure to the atmosphere during the period of injection. Mice displayed ruffled hair within 24 h and began to die 3 days after injection. The numbers of animals dead 6 days after injection of 7×10^9 to 9×10^9 bacterial cells were 13 of 17 with W83, 5 of 13 with 4351, and 1 of 4 with EM23 (Fig. 4 and Table 2). The difference in lethality between W83 and the mutant strains was significant, as determined by Fisher's probability test ($P < 0.05$). There was no significant difference in lethality between the two mutants. All animals that had survived the first 6 days after injection remained alive during the entire observation period of 3 weeks.

Mice challenged with W83 or mutant strains displayed the following macroscopic findings. (i) Mice exhibited no severe lesions at the sites of injection on the dorsal surfaces, except for redness. (ii) Mice developed abscesses on the abdomens 2 days after injection. Within 1 day of abscess appearance, the abscesses ruptured, and drainage and hemorrhage occurred, resulting in ulcer formation. Sixteen of the 17 W83-challenged animals displayed widespread abscesses or ulcerative lesions covering the abdomens. Among the mutant-challenged animals, 6 of 13 injected with 4351 and 4 of 4 injected with EM23 developed similar extensive lesions on the abdomens. The frequencies of extensive lesions caused by W83 and by mutant strains were significantly different ($P < 0.05$) (Table 2). (iii)

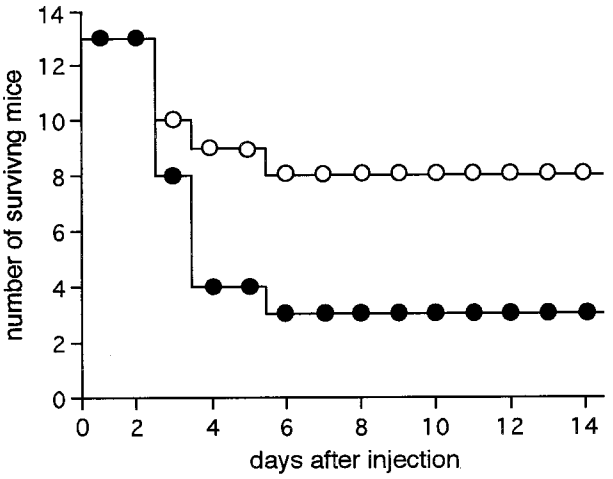

FIG. 4. Number of mice surviving after injection of W83 (●) and *dpp*-deficient mutant 4351 (○). Data represent the sum of three experiments (experiments 1, 2, and 3 in Table 2).

Seven mice injected with 4351 survived throughout the observation period with only localized lesions or with no apparent pathological changes (Table 2). In contrast, one mouse injected with W83 exhibited no abscess on the abdomen but developed severe expansion of the abdomen (Table 2), leading to death in 3 days. Autopsy of this animal revealed that an intestinal protrusion had penetrated through a hole in the peritoneum to reach the subcutaneous region. (iv) Two W83-injected mice and one 4351-challenged animal developed secondary extensive lesions in the thoracic regions within 4 days. (v) Finally, among the surviving animals, one mouse challenged with W83 and three mice challenged with 4351, small ulcerative lesions scattered over several places on the bodies, such as the axillary regions and/or articulations, were found in addition to abscesses on the abdomens.

An increase in body weight was observed in 4351-injected mice at 6 days after injection, while it took longer (more than 2 weeks) for the body weight of W83-injected mice to increase

TABLE 2. Lesions induced by injection of W83 or *dpp*-deficient mutants

Expt (dose/mouse)	Strain	No. of mice/no. tested		
		With the following lesions		Dead
		Extensive[a]	Localized[b]	
1 (8×10^9)	W83	4/4		4/4
	4351	3/4	1/4	2/4
2 (8×10^9)	W83	4/4		2/4
	4351	1/4	2/4	1/4
3 (9×10^9)	W83	4/5[c]		4/5
	4351	2/5	3/5	2/5
4[d] (7×10^9)	W83	4/4		3/4
	EM23	4/4		1/4

[a] Covering the abdominal area.
[b] On the abdomen.
[c] One mouse did not develop an extensive lesion but exhibited severe expansion of the abdomen.
[d] The extent of lesion expansion caused by EM23 was much smaller than that caused by W83.

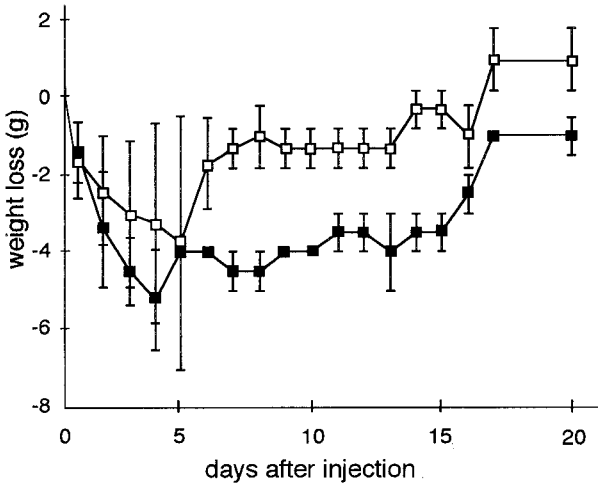

FIG. 5. Average loss of body weight after injection of W83 (■) and *dpp*-deficient mutant 4351 (□) in experiment 2 of Table 2. Zero grams on the *y* axis is the average weight of mice just before injection. Error bars indicate standard deviations.

in experiment 2 (Table 2 and Fig. 5). Similar results were obtained in other experiments shown in Table 2. In concurrence with weight gain, surviving mice showed scarring of ulcerative lesions. Lesions caused by W83 healed much more slowly than those caused by the mutants. The findings indicated that mice challenged with the mutants exhibited faster recovery from the infection than those injected with W83.

DISCUSSION

We purified DPPIV from the soluble fraction of *P. gingivalis* W83 and obtained 19 μg from 1.5 liters of bacterial culture. The amount of protein that we obtained was much higher than that in a previous report (8 μg from 10 liters) in which freezing-thawing had not been carried out (26). *P. gingivalis* cells could be broken more readily by sonication after freezing-thawing.

The secondary or higher structure of bacterial DPPIV has not been clarified. However, the primary structure of *P. gingivalis* DPPIV deduced from the DNA sequence revealed high homology with those of eukaryotic DPPIVs, especially in the C-terminal catalytic region. Furthermore, by site-directed mutagenesis, the amino acid residues Ser593, Asp668, and His700 were suggested to participate in catalytic activity. It was suggested that Ser593 is a catalytic Ser residue and that the three residues form a catalytic triad, as previously described for mouse DPPIV (9).

Some enzymatic properties of *P. gingivalis* DPPIV were similar to those of eukaryotic DPPIVs. First, the enzyme is composed of a homodimer, as proved by gel filtration HPLC. Second, recombinant *P. gingivalis* DPPIV cleaved peptides that correspond to the N-terminal portion of the CC chemokines RANTES and MCP1, just as human DPPIV did, as demonstrated by reverse-phase HPLC. From the results, *P. gingivalis* DPPIV is likely to remove dipeptides from some of the CC chemokines, as described for human DPPIV (3, 40). Further investigation is necessary to confirm the cleavage of CC chemokines by *P. gingivalis* DPPIV.

In contrast to that of human DPPIV, binding of *P. gingivalis* DPPIV to bovine ADA was not observed by two different experimental methods, gel electrophoresis followed by Western blotting and ADA affinity column chromatography. Amino acid residues Leu340, Val341, Ala342, and Arg343 of human DPPIV were identified to be essential for binding to bovine ADA (11). The corresponding amino acids of *P. gingivalis* DPPIV would be Leu342, Val343, Pro344, and Lys345 when aligned; these residues do not differ greatly from the residues of human DPPIV. Other amino acids which are not conserved in *P. gingivalis* DPPIV may be required to form the binding domain for bovine ADA. For example, when Glu332-Ser333-Ser334-Gly335-Arg336 in human DPPIV was substituted with Lys-Ile-Asn-Leu-Thr, ADA binding of the mutant human DPPIV decreased significantly (11). Another possible explanation for the difference between *P. gingivalis* DPPIV and human DPPIV is species specificity of binding to ADA. Bacterial DPPIV may bind to bacterial ADA rather than to eukaryotic ADA. The fact that mouse DPPIV did not bind to bovine ADA (11) supports this supposition.

The N-terminal amino acid sequence of purified DPPIV could not be determined, presumably because the N terminus of the purified protein is blocked. The enzyme seems to be localized on the outside of the cytoplasm, since it possesses a typical signal sequence. Eukaryotic DPPIV has been reported to be localized on membranes such as the T-cell surface (3, 11, 22, 27, 38, 43), both bile canalicular and sinusoidal membranes of hepatocytes (33), and the membrane of the brush border of the small intestine and kidneys (3). *P. gingivalis* DPPIV is most likely to be localized on the outer membrane, as suggested by the following results. The enzymatic activity of intact whole cells was comparable to that of the sonic extract. Furthermore, DPPIV activity of intact whole cells was reduced to an extent similar to that of the sonic extract after protease treatment (unpublished data). DPPIV activity in the soluble fraction, comprising more than 90% of the total activity, was likely to be derived from the outer membrane. DPPIV may bind loosely to the outer membrane and be released by sonication.

Taken together, the results indicate that *P. gingivalis* DPPIV and eukaryotic DPPIV share several properties, such as primary structure, catalytic triad, dimer formation, substrate specificity, and localization. The similarity between *P. gingivalis* DPPIV and eukaryotic DPPIV led us to predict that *P. gingivalis* DPPIV has significant pathological roles. Eukaryotic DPPIV has been thought to be associated with pathogenesis in several aspects: (i) DPPIV cleaved CC chemokines, and the resulting truncated chemokines exhibited reduced activity as chemoattractants for monocytes and less efficient induction of a Ca^{2+} response in monocytes (3, 40); (ii) DPPIV removed dipeptide from stromal cell-derived factor 1, and both lymphocyte chemotactic activity and inhibitory activity against human immunodeficiency virus infection disappeared after digestion (3, 31); (iii) DPPIV expressed on the lung endothelial membrane was shown to mediate adhesion and metastasis of breast cancer cells through binding to extracellular matrix proteins (6); (iv) suppression of T cells by human immunodeficiency virus type 1 Tat protein occurred through binding of Tat to DPPIV (3, 14, 45); and (v) finally, DPPIV is implicated in the development of diabetes by cleaving glucose-dependent insulinotropic polypeptide and glucagon-like peptide 1 (3). We suppose that *P. gingivalis* DPPIV has similar functions in developing and maintaining periodontitis. *P. gingivalis* DPPIV may also possess cleaving activity for CC chemokines and stromal cell-derived factor 1, as mentioned above, which reduces the chemotactic activity of monocytes or lymphocytes. This enzyme may also participate in the interaction of *P. gingivalis* and extracellular matrix proteins.

To investigate whether *P. gingivalis* DPPIV participates in the virulence of the bacteria, we constructed two types of DPPIV-deficient mutants: null mutants with most of the *dpp*

gene deleted and an insertion mutant. The virulence of wild-type W83 was significantly greater than that of the mutants, as judged by abscess formation, lethality, and recovery from the infection (Fig. 4 and 5 and Table 2). The present results suggest that DPPIV is a virulence factor, although the relationship between the mouse abscess model and periodontitis still remains to be determined. Thus, we are currently carrying out a histopathological study of the lesions and organs obtained from mice that died during the present study, mice that survived until the end of the study, or all mice 3 days after injection.

Banbula et al. (4) have recently reported the purification and DNA sequence of PtpA from *P. gingivalis*, which cleaves X-Y-Pro from the N termini of peptides. The primary structure of PtpA is highly homologous to that of *P. gingivalis* DPPIV. The consensus sequence around the active Ser commonly found in DPPIVs, Gly-Trp-Ser-Tyr-Gly, is conserved, and the putative catalytic triad, Ser-Asp-His, is found in PtpA. In addition, some enzymatic properties of DPPIV and PtpA are similar: molecular weight, localization on the cell surface, and possible blockage of the N terminus. PtpA and DPPIV of *P. gingivalis* may have developed from a common ancestor.

Three additional genes encoding proteases homologous with DPPIV were found in the *P. gingivalis* genome (4). The possibility that the gene products, if expressed, have enzymatic activity has been suggested (4). However, the proteases are not members of the S9 oligopeptidase family to which DPPIVs belong, since the proteases do not have the consensus sequence around the active Ser of DPPIV. Furthermore, these proteases may not function like DPPIV, at least in rich medium, since measurable DPPIV activity was not detected in the deletion mutants and the insertion mutant in this study.

ACKNOWLEDGMENTS

We thank Yasuhiro Watanabe for providing human DPPIV and anti-ADA antibody and Takaaki Aoba for heartfelt understanding.

This work was supported by grants-in-aid for scientific research 07457071 and 08307004 from the Ministry of Education, Science, Culture and Sports, Japan.

REFERENCES

1. **Abiko, Y., M. Hayakawa, S. Murai, and H. Takiguchi.** 1985. Glycylprolyl dipeptidylaminopeptidase from *Bacteroides gingivalis*. J. Dent. Res. **64:**106–111.
2. **Anna-Arriola, S. S., and I. Herskowitz.** 1994. Isolation and DNA sequence of the *STE13* gene encoding dipeptidyl aminopeptidase. Yeast **10:**801–810.
3. **Augustyns, K., G. Bal, G. Thonus, A. Belyaev, X. M. Zhang, W. Bollaert, A. M. Lambeir, C. Durinx, F. Goosens, and A. Haemers.** 1999. The unique properties of dipeptidyl-peptidase IV (DPPIV/CD26) and the therapeutic potential of DPPIV inhibitors. Curr. Med. Chem. **6:**311–327.
4. **Banbula, A., P. Mak, M. Bugno, J. Silberring, A. Dubin, D. Nelson, J. Travis, and J. Potempa.** 1999. Prolyl tripeptidyl peptidase from *Porphyromonas gingivalis*. A novel enzyme with possible pathological implications for the development of periodontitis. J. Biol. Chem. **274:**9246–9252.
5. **Brenner, S.** 1988. The molecular evolution of genes and proteins: a tale of two serines. Nature **334:**528–530.
6. **Cheng, H.-C., M. Abdel-Ghany, R. C. Elble, and B. U. Pauli.** 1998. Lung endothelial dipeptidyl peptidase IV promotes adhesion and metastasis of rat breast cancer cells via tumor cell surface-associated fibronectin. J. Biol. Chem. **273:**24207–24215.
7. **Darmoul, D., M. Lacasa, L. Baricault, D. Marguet, C. Sapin, P. Trotot, A. Barbat, and G. Trugnan.** 1992. Dipeptidyl peptidase IV (CD26) gene expression in enterocyte-like colon cancer cell lines HT-29 and Caco-2. J. Biol. Chem. **267:**4824–4833.
8. **Date, T., K. Tanihara, and N. Numura.** 1990. Construction of *Escherichia coli* vectors for expression and mutagenesis: synthesis of human c-Myc protein that is initiated at a non-AUG codon in exon 1. Gene **90:**141–144.
9. **David, F., A.-M. Bernard, M. Pierres, and D. Marguet.** 1993. Identification of serine 624, aspartic acid 702, and histidine 734 as the catalytic triad residues of mouse dipeptidyl-peptidase IV (CD26). J. Biol. Chem. **268:** 17247–17252.
10. **De Meester, I., G. Vanhoof, A.-M. Lambeir, and S. Scharpé.** 1996. Use of immobilized adenosine deaminase (EC 3.5.4.4) for the rapid purification of native human CD26/dipeptidyl peptidase IV (EC 3.4.14.5). J. Immunol. Methods **189:**99–105.
11. **Dong, R.-P., K. Tachibana, M. Hegen, Y. Munakata, D. Cho, S. F. Schlossman, and C. Morimoto.** 1997. Determination of adenosine deaminase binding domain on CD26 and its immunoregulatory effect on T cell activation. J. Immunol. **159:**6070–6076.
12. **Fletcher, H. M., H. A. Schenkein, R. M. Morgan, K. A. Bailey, C. R. Berry, and F. L. Macrina.** 1995. Virulence of a *Porphyromonas gingivalis* W83 mutant defective in the *prtH* gene. Infect. Immun. **63:**1521–1528.
13. **Genco, C. A., T. Van Dyke, and S. Amar.** 1998. Animal models for *Porphyromonas gingivalis*-mediated periodontal disease. Trends Microbiol. **6:**444–449.
14. **Gutheil, W. G., M. Subramanyam, G. R. Flentke, D. G. Sanford, E. Munoz, B. T. Huber, and W. W. Bachovchin.** 1994. Human immunodeficiency virus 1 Tat binds to dipeptidyl aminopeptidase IV (CD26): a possible mechanism for Tat's immunosuppressive activity. Proc. Natl. Acad. Sci. USA **91:**6594–6598.
15. **Holt, S. C., J. Ebersole, J. Felton, M. Brunsvold, and K. S. Kornman.** 1988. Implantation of *Bacteroides gingivalis* in nonhuman primates initiates progression of periodontitis. Science **239:**55–57.
16. **Iwaki-Egawa, S., Y. Watanabe, Y. Kikuya, and Y. Fujimoto.** 1998. Dipeptidyl peptidase IV from human serum: purification, characterization, and N-terminal amino acid sequence. J. Biochem. **124:**428–433.
17. **Kabashima, T., T. Yoshida, K. Ito, and T. Yoshimoto.** 1995. Cloning, sequencing, and expression of the dipeptidyl peptidase IV gene from *Flavobacterium meningosepticum* in *Escherichia coli*. Arch. Biochem. Biophys. **320:** 123–128.
18. **Kiyama, M., M. Hayakawa, T. Shiroza, S. Nakamura, A. Takeuchi, Y. Masamoto, and Y. Abiko.** 1998. Sequence analysis of the *Porphyromonas gingivalis* dipeptidyl peptidase IV gene. Biochim. Biophys. Acta **1396:**39–46.
19. **Kunkel, T. A.** 1985. Rapid and efficient site-specific mutagenesis without phenotypic selection. Proc. Natl. Acad. Sci. USA **82:**488–492.
20. **Laemmli, U. K.** 1970. Cleavage of structural proteins during the assembly of the head of bacteriophage T4. Nature **227:**680–685.
21. **Lambeir, A.-M., J. F. Díaz Pereira, P. Chacón, G. Vermeulen, K. Heremans, B. Devreese, J. Van Beeumen, I. De Meester, and S. Scharpé.** 1997. A prediction of DPP IV/CD26 domain structure from a physico-chemical investigation of dipeptidyl peptidase IV (CD26) from human seminal plasma. Biochim. Biophys. Acta **1340:**215–226.
22. **Marguet, D., A.-M. Bernard, I. Vivier, D. Darmoul, P. Naquet, and M. Pierres.** 1992. cDNA cloning for mouse thymocyte-activating molecule. J. Biol. Chem. **267:**2200–2208.
23. **Mayo, B., J. Kok, K. Venema, W. Bockelmann, M. Teuber, H. Reinke, and G. Venema.** 1991. Molecular cloning and sequence analysis of the X-prolyl dipeptidyl aminopeptidase gene from *Lactococcus lactis* subsp. *cremoris*. Appl. Environ. Microbiol. **57:**38–44.
24. **Miller, V. L., and J. J. Mekalanos.** 1988. A novel suicide vector and its use in construction of insertion mutations: osmoregulation of outer membrane proteins and virulence determinants in *Vibrio cholerae* requires *toxR*. J. Bacteriol. **170:**2575–2583.
25. **Misumi, Y., Y. Hayashi, F. Arakawa, and Y. Ikehara.** 1992. Molecular cloning and sequence analysis of human dipeptidyl peptidase IV, a serine proteinase on the cell surface. Biochim. Biophys. Acta **1131:**333–336.
26. **Miyauchi, T., M. Hayakawa, and Y. Abiko.** 1989. Purification and characterization of glycylprolyl aminopeptidase from *Bacteroides gingivalis*. Oral Microbiol. Immunol. **4:**222–226.
27. **Morimoto, C., and S. F. Schlossman.** 1998. The structure and function of CD26 in the T-cell immune response. Immunol. Rev. **161:**55–70.
28. **Nakayama, K., T. Kadowaki, K. Okamoto, and K. Yamamoto.** 1995. Construction and characterization of arginine-specific cysteine proteinase (arg-gingipain)-deficient mutants of *Porphyromonas gingivalis*. J. Biol. Chem. **270:** 23619–23626.
29. **Nakayama, K., F. Yoshimura, T. Kadowaki, and K. Yamamoto.** 1996. Involvement of arginine-specific cysteine proteinase (arg-gingipain) in fimbriation of *Porphyromonas gingivalis*. J. Bacteriol. **178:**2818–2824.
30. **Nardi, M., M.-C. Chopin, A. Chopin, M.-M. Cals, and J.-C. Gripon.** 1991. Cloning and DNA sequence analysis of an X-prolyl dipeptidyl aminopeptidase gene from *Lactococcus lactis* subsp. *lactis* NCDO 763. Appl. Environ. Microbiol. **57:**45–50.
31. **Ohtsuki, T., O. Hosono, H. Kobayashi, Y. Munakata, A. Souta, T. Shioda, and C. Morimoto.** 1998. Negative regulation of the anti-human immunodeficiency virus and chemotactic activity of human stromal cell-derived factor 1α by CD26/dipeptidyl peptidase IV. FEBS Lett. **431:**236–240.
32. **Potempa, J., N. Pavloff, and J. Travis.** 1995. *Porphyromonas gingivalis*: a protease/gene accounting audit. Trends Microbiol. **3:**430–434.
33. **Piazza, G. A., H. M. Callanan, J. Mowery, and D. C. Hixson.** 1989. Evidence for a role of dipeptidyl peptidase IV in fibronectin-mediated interactions of hepatocytes with extracellular matrix. Biochem. J. **262:**327–334.
34. **Pugsley, A. P.** 1993. The complete general secretory pathway in gram-negative bacteria. Microbiol. Rev. **57:**50–108.
35. **Roberts, C. J., G. Pohlig, J. H. Rothman, and T. H. Stevens.** 1989. Structure,

biosynthesis, and localization of dipeptidyl aminopeptidase B, an integral membrane glycoprotein of the yeast vacuole. J. Cell Biol. **108:**1363–1373.
36. **Sambrook, J., E. F. Fritsch, and T. Maniatis.** 1989. Molecular cloning: a laboratory manual, 2nd ed. Cold Spring Harbor Laboratory Press, Cold Spring Harbor, N.Y.
37. **Schenkein, H. A., H. M. Fletcher, M. Bodnar, and F. L. Macrina.** 1995. Increased opsonization of a *prtH*-defective mutant of *Porphyromonas gingivalis* W83 is caused by reduced degradation of complement-derived opsonins. J. Immunol. **154:**5331–5337.
38. **Tanaka, T., D. Camerini, B. Seed, Y. Torimoto, N. H. Dang, J. Kameoka, H. N. Dahlberg, S. F. Schlossman, and C. Morimoto.** 1992. Cloning and functional expression of the T cell activation antigen CD26. J. Immunol. **149:**481–486.
39. **Tokuda, M., T. Karunakaran, M. Duncan, N. Hamada, and H. Kuramitsu.** 1998. Role of arg-gingipain A in virulence of *Porphyromonas gingivalis*. Infect. Immun. **66:**1159–1166.
40. **Van Coillie, E., P. Proost, I. Van Aelst, S. Struyf, M. Polfliet, I. De Meester, D. J. Harvey, J. Van Damme, and G. Opdenakker.** 1998. Functional comparison of two human monocyte chemotactic protein-2 isoforms, role of the amino-terminal pyroglutamic acid and processing by CD26/dipeptidyl peptidase IV. Biochemistry **37:**12672–12680.
41. **Vesanto, E., K. Savijoki, T. Rantanen, J. L. Steele, and A. Palva.** 1995. An X-prolyl dipeptidyl aminopeptidase (*pepX*) gene from *Lactobacillus helveticus*. Microbiology **141:**3067–3075.
42. **Vieira, J., and J. Messing.** 1982. The pUC plasmids, an M13mp7-derived system for insertion mutagenesis and sequencing with synthetic universal primers. Gene **19:**259–268.
43. **von Bonin, A., J. Hühn, and B. Fleisher.** 1998. Dipeptidyl-peptidase IV/CD26 on T cells: analysis of an alternative T-cell activation pathway. Immunol. Rev. **161:**43–53.
44. **von Heijne, G.** 1986. A new method for predicting signal sequence cleavage sites. Nucleic Acids Res. **14:**4683–4690.
45. **Wrenger, S., T. Hoffmann, J. Faust, C. Mrestani-Klaus, W. Brandt, K. Neubert, M. Kraft, S. Olek, R. Frank, S. Ansorge, and D. Reinhold.** 1997. The N-terminal structure of HIV-1 Tat is required for suppression of CD26-dependent T cell growth. J. Biol. Chem. **272:**30283–30288.

Editor: D. L. Burns